Influence of Viscosity and Non-linearities in Predicting Motions of a Wind Energy Offshore Platform In Regular Waves

José del Águila Ferrandis

May 15, 2019

Massachusetts Institute of Technology

Codes Used

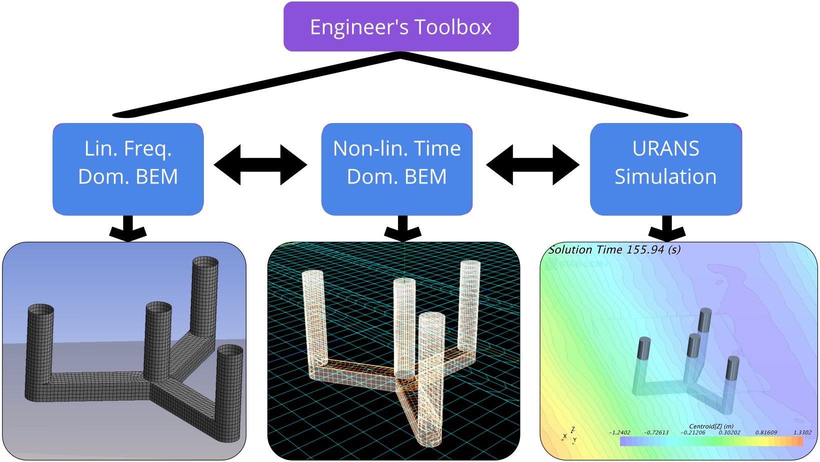
Engineer's Toolbox
Lin. Freq. Dom. BEM
Non-lin. Time Dom. BEM
URANS Simulation
Solution Time 155.94 (s)
Centroid[Z] (m)
-1.2402
-0.72613
-0.21206
0.30202
0.81609
1.3302

Challenges in Solving the Seakeeping Problem

- Numerical models give the possibility of **full scale** prediction.
- Froude & Reynolds incomplete **similarity**.
- Viscous codes allow for better accuracy at **resonance**.
- Viscous codes can also calculate **large non-linear motions & wave breaking**.

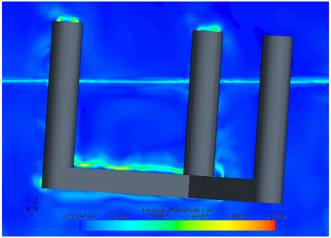

Figure: 3DOF extreme weather

Linear Frequency Domain BEM

Solve Laplace Equation:

$$\nabla^2(\phi) = 0$$

Given the BCs:

$$g\eta + \frac{\partial \phi}{\partial t} = 0 \quad \text{at} \quad z = 0$$
$$\frac{\partial \eta}{\partial t} - \frac{\partial \phi}{\partial z} = 0 \quad \text{at} \quad z = 0$$
$$\frac{\partial \phi}{\partial z} = 0 \quad \text{at} \quad z = -h$$

Potential Decomposed:

$$\phi = \phi_D + \phi_R = \phi_I + \phi_S + \phi_R$$

Eq. Dipole Moments:

$$\begin{pmatrix} 2\pi \\ 4\pi \end{pmatrix} \phi_D(\mathbf{x}) + \iint_{S_b} \phi_D G_{n_\xi} dS_\xi = 4\pi\phi_I(\mathbf{x})$$

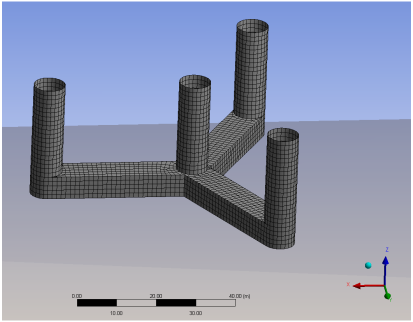

Figure: Mesh in freq. dom. BEM.

Non-linear Time Domain BEM

- During the non-linear calculations, the intersection between the free surface and the platform is calculated. B-splines used to represent perturbation potential in the wet hull parametric space.
- The kinematic and dynamic free surface conditions are both expanded in a Taylor-series about the base flow:

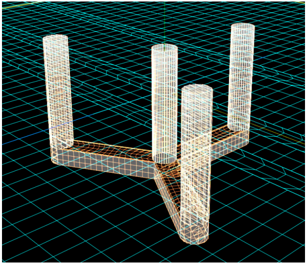

Figure: Mesh example.

$$\zeta \left(\frac{\partial}{\partial t} - (\vec{U} - \nabla \Phi) \cdot \nabla \right) = \frac{\partial^2 \Phi}{\partial z^2} \zeta + \frac{\partial \phi}{\partial z}$$

$$\phi \left(\frac{\partial}{\partial t} - (\vec{U} - \nabla \Phi) \cdot \nabla \right) = -g \left(\zeta + z_m \right) + \left(\vec{U} \cdot \nabla \Phi - \frac{1}{2} \nabla \phi \cdot \nabla \phi \right)$$

Time-Domain Fully Viscous Model - URANS - VOF

Volume of Fluid Method. Averaged continuity and momentum equations for incompressible fluids.

$$\frac{\partial\left(\overline{\rho u_i}\right)}{\partial x_i} = 0$$

$$\frac{\partial\left(\overline{u u_i}\right)}{\partial x_j}\left(\rho\overline{u}_i\overline{u}_j + \rho\overline{u_i' u_j'}\right) = \frac{\partial\overline{p}}{\partial x_i} + \frac{\partial\overline{\tau}_{ij}}{\partial x_j}$$

$$\overline{\tau}_{ij} = \mu\left(\frac{\partial\overline{u}_i}{\partial x_j} + \frac{\partial\overline{u}_j}{\partial x_i}\right)$$

Simple Implicit Time Advancing Scheme is used.

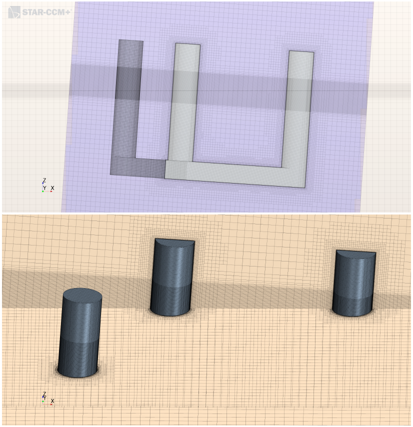

Figure: Mesh in URANS.

Mesh & Time-step Convergence.

- Values of **y+** $\sim$ **55** on average $\longleftrightarrow$ SST-Menter-k-ω.
- Volume of fluid Method (**VOF**).
- **DFBI + Overset grids** to simulate Heave and Pitch Motions (head seas).
- Time-step given by **Courant Number** on the free surface.

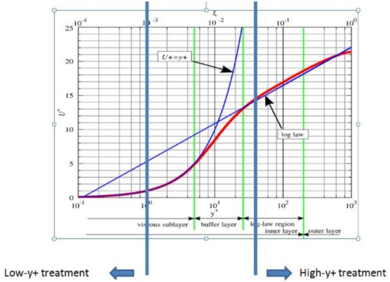

Figure: High Wall y+ treatment for high y+ numbers.

Mesh & Time-step Convergence.

- Wave probe in the undisturbed region. The signal obtained is compared to the theoretical profile of a **1st order Stokes wave**.
- Discrepancies are due to **surface capturing technique** and mesh resolution across the free surface.
- To account for this, we consider the wave amplitude obtained by applying a Fast Fourier Transform to the **numerical wave profile**.

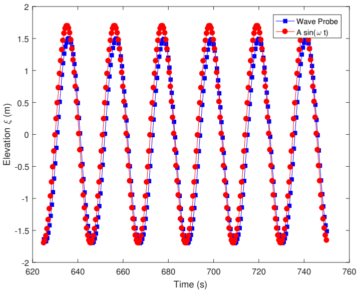

Figure: Numerical wave profile corresponds to the blue line.

Mesh & Time-step Convergence.

Mesh Sensitivity Analysis–RAO Variation												
T_w	18s				19s				19.5s			
Mesh	e_{33}	e_{55}	cells	y+	e_{33}	e_{55}	cells	y+	e_{33}	e_{55}	cells	y+
MR1	29%	5%	2e6	424	9%	11%	2e6	377	9%	6%	1e6	356
MR2	30%	4%	3e6	317	7%	9%	3e6	315	11%	6%	2e6	305
MR3	8%	1%	6e6	167	4%	1%	6e6	157	2%	2%	3e6	137
Final	0%	0%	7e6	49	0%	0%	8e6	50	0%	0%	4e6	48

T_w	20s				21s				30s			
Mesh	e_{33}	e_{55}	cells	y+	e_{33}	e_{55}	cells	y+	e_{33}	e_{55}	cells	y+
MR1	3%	10%	1e6	361	0%	15%	1e6	351	0%	5%	1e6	331
MR2	3%	10%	2e6	303	1%	11%	2e6	280	1%	2%	2e6	160
MR3	2%	3%	3e6	131	1%	4%	3e6	119	0%	0%	3e6	105
Final	0%	0%	5e6	46	0%	0%	5e6	40	0%	0%	4e6	55

Table: Results of the convergence of the RAOs in a mesh sensitivity analysis considering **4 levels of refinement**. Convergence is quickly reached in all wave periods except for $T_w = 18s$. For this reason mesh *Final* is used.

Mesh & Time-step Convergence.

T_w	λ_w	H_w	T_{step}
10.00	156.131	2 × 0.771	0.012
13.00	263.861	2 × 1.303	0.0155
15.00	351.293	2 × 1.735	0.0179
16.00	399.702	2 × 1.971	0.0190
16.73	437.523	2 × 2.160	0.0199
18.00	505.864	2.498	0.023
19.00	563.633	2.783	0.023
19.50	593.688	2.932	0.023
20.00	624.524	3.084	0.024
21.00	688.538	3.400	0.025
30.00	1405.179	6.939	0.036

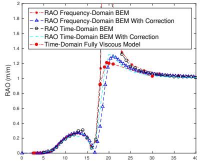

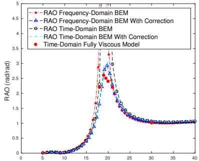

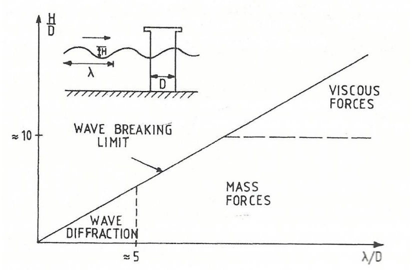

Figure: Sea Loads, Faltinsen.

Cross-validation of Numerical Results

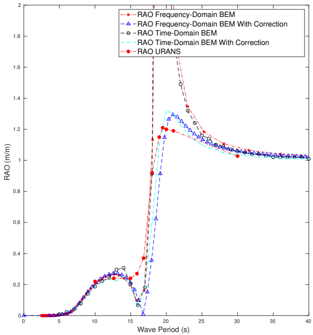

(a) Heave motion RAOs.

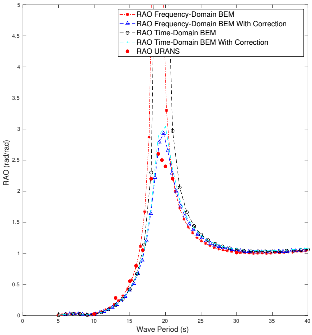

(b) Pitch motion RAOs.

Figure: Additional damping is introduced in a second set BEM simulations. Empirical damping selected given URANS (6.25%,6.5%).

- Limitation of potential flow models in motions for waves having periods close to the **natural & cancellation frequencies**.
- Corrections coefficients can be obtained from URANS.
- **computational burden**: 1-175-700,000.
- Very similar predictions for small motions only requiring URANS near the resonance and cancellation period.

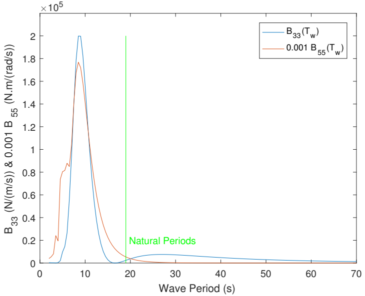

Figure: B_{33} and B_{55} radiation damping coefficients.